Journal of Earth Sciences and Geotechnical Engineering, Vol. 9, No. 3, 2019, 117-132
ISSN: 1792-9040 (print version), 1792-9660 (online)
Scientific Press International Limited

Degradation Mechanisms in Smectitic Clay for Isolating Radioactive Waste

Roland Pusch[1], Jörn Kasbohm[2] and Thao Hoang-Minh[3]

Abstract

Most of the proposed techniques for chemical shielding of radioactive waste implies use of smectite clay, which degrades according to a well-known scheme. Since such "buffer" clay has to serve for many thousands of years, the mechanisms in the unavoidable long-term degradation process must be understood and accounted for as described in the paper. In addition to conversion of smectite to non-expandable minerals cementation by precipitation of siliceous matter created in the degradation process is of concern since it can reduce the self-sealing capacity of desiccated or mechanically damaged clay.

Keywords: Smectite clays, diffractogram, radioactive wastes, montmorillonite, XRD, TEM, Holmehus clay.

[1] Lulea Technical University, Lulea, Sweden
[2] Greifswald University, Greifswald, Germany
[3] VNU University of Science, Vietnam National University, Hanoi, Vietnam

Article Info: *Received:* June 5, 2019. *Revised:* August 23, 2019.
Published online: September 10, 2019.

1. Introduction

Smectite clays are proposed as chemical/mineralogical buffer in repositories for radioactive waste requiring long-term service. This is threatened by conversion to non-expandable clay minerals as discussed in the present paper.
A fundamental general chemical process is the empirical reaction expressed by Equation (1):

$$S + (Fk + Mi) = I + Q + Chl \quad (1)$$

where S denotes smectite, Fk K-feldspars, Mi micas, Q quartz, and Chl chlorite.

The reaction formula is a generalization and says nothing about the ways in which the conversion to illite takes place and what the conditions are. Diagenetic formation of illite and interstratified I/S (illite/smectite) was established in The Clay Mineral Society already in the sixties implying a layer-by-layer altering mechanism by which smectite layers are converted to illite layers. Nadeau has shown that the conversion can have the form of dissolution of smectite and precipitation of (20 Å) illite particles in intimate association with smectite particles (Nadeau et al, 1985). A most important parameter that does not appear explicitly in the equation is the access to potassium. It is generally believed that it determines the rate of conversion and that the amount of illite formed will be insignificant where the concentration of this element is very low. This may not be the case, however, since potassium can originate from dissolved I/S particles, implying cannibalization as suggested by Pollastro (1985). Naturally, illite formation is slower in very dense smectite clay than in soft clay, like bore muds, since the migration of all elements required for neo-crystallization takes place by very slow diffusion.
A guiding series of experiments made in a joint French/Swedish R&D project in the seventy/eighties is still a mine of information. Cylindrical 7 cm long MX-80 samples with a dry density of 1650 kg/m^3 were confined in cells with an iron plate at the heated end and a water saturated filter at the opposite one (Pusch et al, 1993). Weakly brackish water with Na as dominant cation and very little potassium (<10 ppm) was circulated through the filter that was kept at 90^{o}C. The iron plate was heated to 130^{o}C during the 1-year experiments, yielding a thermal gradient of about 6^{o}C/cm. The solution was pressurized to 1.5 MPa. In one of the tests a gamma radiation dose of about 3E7 Gy acted on the iron plate, the adsorbed radiation dose being 3972 Gy/h at the hot plate contact, around 700 Gy/h at half length of the sample, and 456 Gy/h at the coldest end. The investigation of the samples comprised XRD analysis (Figure 1), electron microscopy with EDX, chemical analysis, infrared spectrometry, and CEC determination. The results can be summarized as follows (cf. Figure 1):

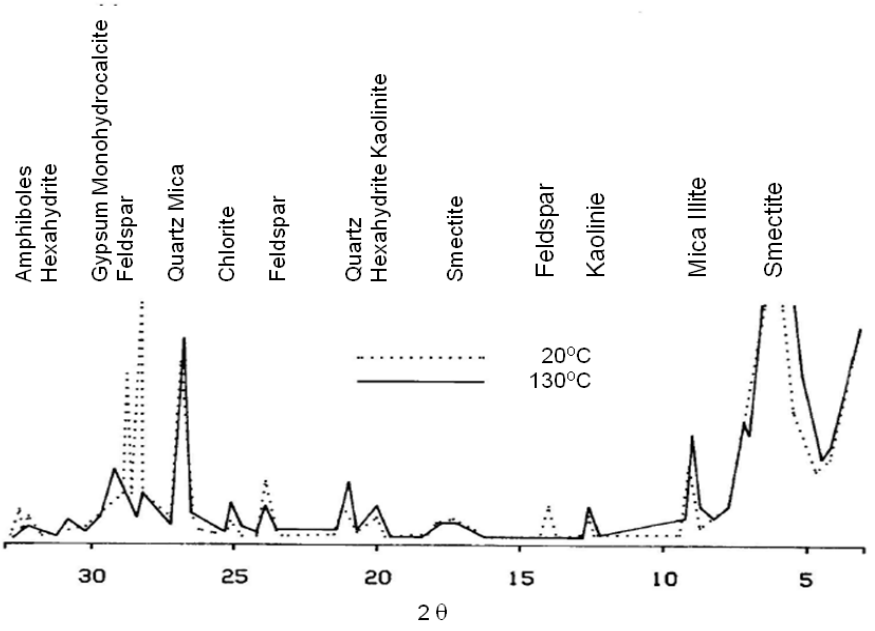

Figure 1: Schematic diffractograms of the reference MX-80 sample (20ºC) and the most heated part of the hydrothermally tested sample (130ºC). Feldspars, amphibole, some of the quartz and smectite disappeared in the hot part (Pusch et al, 1993).

The analyses reported in Table 1 showed that there was nearly no difference between the sample exposed to γ radiation and the one that was not irradiated, except that Fe migrated from the iron plate into the clay somewhat quicker under radiation. Comparison with virgin MX-80 clay showed that hydrothermal treatment with and without radiation gave insignificant chemical changes, which was also supported by CEC data. They showed that untreated MX-80 had CEC=99 meq/100 g while the most strongly heated and radiated clay had CEC=93 meq/100 g. However, creep testing at room temperature of samples at various distances from the hottest end showed obvious stiffening (Figure 2). Thus, the shear strain of the sample exposed to 130ºC was about 3 times smaller than of the one heated to 90ºC.

Table 1: Changes in one year long hydrothermal tests of MX-80.

Treatment	125-130ºC	115-120ºC	105-110ºC	90-95ºC
Hydrothermal without radiation	M - F --- Chl+ G ++ K ++ Q + I +	M – F -- Chl + G +++ K + Q + I 0	M 0 F - Chl 0 G + K 0 Q 0 I 0	M 0 F - Chl 0 G+ K - Q 0 I 0
M=Montmorillonite, F=Feldspars, G=Gypsum, Q=Quartz, K=Kaolinite, Chl=Chlorite, I=Illite. +++ means strong increase, ++ significant increase, + slight increase, --- strong loss, -- significant loss, - slight loss. 0 means no change.				

2. Grindrod/Takase's model

In contrast to the conventional Reynold-type models, the one proposed by Grindrod and Takase (Grindrod and Takase, 1993) considers dissolution and precipitation of phyllosilicates by taking $O_{10}(OH)_2$ as a basic unit and defines a general formula for smectite and illite:

$$X_{0.35}\,Mg_{0.33}\,Al_{1.65}\,Si_4O_{10}\,(OH)_2 \text{ and } K_{0.5\text{-}0.75}\,Al_{2.5\text{-}2.75}\,Si_{3.25\text{-}3.5}\,O_{10}(OH)_2 \quad (2)$$

where X is the interlamellar absorbed cation (Na) for Na montmorillonite.

Dissolution takes place according to the following reaction:

$$Na_{0.33}\,Mg_{0.33}\,Al_{1.67}\,Si_4O_{10}(OH)_2 + 6H^+ = 0.33Na + 0.33Mg^{2+} + 1.67Al^{3+} + 4SiO_{2(aq)} + 4H_2O \quad (3)$$

Precipitation takes place according to the following reaction:

$$K\,AlSi_3\,O_{10}\,(OH)_2 = K^+ + 3Al^{3+} + 3\,SiO_2(aq) + 6H_2, \quad (4)$$

(logK being a function of temperature).

The rate of the reaction *r* can be expressed as:

$$r = A \exp(-E_a/RT)(K^+)S^2 \quad (5)$$

where:
A=coefficient
E_a=activation energy for S/I conversion
R=universal gas constant
T=absolute temperature
K^+=potassium concentration in the porewater
S=specific surface area for reaction

The chemical model is coupled with the transport problem in the one-dimensional cylindrical coordinate representing the buffer material. The kinetic reactions are linked with diffusion-dominated transport of the aqueous species, i.e., silica, aluminum, sodium, magnesium, and potassium, to form a set of quasi-nonlinear partial differential equations for the aqueous species and minerals. The modellers made spatial discretising by using a finite difference scheme that provided a set of ordinary differential equations by use of which one can determine the concentration of each aqueous species by solving the mass action equations with the total concentration of the element in question.

The model has been applied to the KBS-3V case (Figure 2) by Grindrod and Takase (cf. Pusch & Yong, 2006), taking the following data as a basis:

- dry density of the smectite buffer = 1700 kg/m^3
- porosity = 0.35,
- montmorillonite fraction by weight = 75 %,
- initial pore water is seawater,
- groundwater is of seawater origin and assumed to be in equilibrium with granite at the specified temperature in the surrounding rock, *e.g.*, 60 ^{o}C during the first 500 years,
- temperature at canister surface = 90^{o}C, temperature at rock wall = 60^{o}C,
- diameter of hole is 1.8m, diameter of canister is 1.0m,
- vertical water flow rate in the 1 cm rock annulus (EDZ) around the hole is 1 mm/day and 1 mm/month, respectively,
- diffusion coefficient of K^+ in the clay is E-9 m^2/s,
- considered time = 500 years

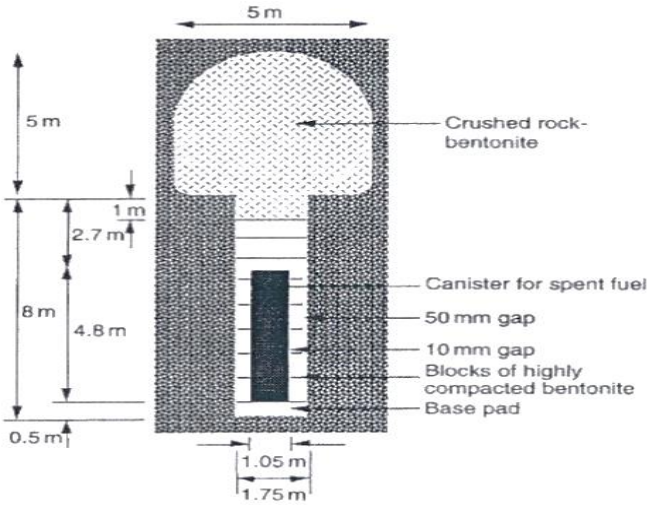

Figure 2: Section of KBS-3V proposed by Swedish Nuclear Fuel and Waste Management.

Assuming the radial thermal gradient (about 0.75°C per cm radial distance from the canister surface) to be constant during the considered time period, silica will be released and transported from the hottest to the coldest part of the clay buffer. Despite the conservative assumption of constant thermal gradient in the first 500 years, the model shows that no illite will be formed this early. However, cooling will change this as documented by considering a period after 500 years with linear temperature drop with time to 25°C after 10,000 years (Pusch, 2008). Silicification and illite formation will hence take place, the first mentioned being illustrated in Figure 3, from which it is concluded that precipitation of quartz will take place within about 0.1 m from the rock wall. The possibility of amorphous silica precipitation is believed to depend very much on the time scale of cooling relative to that of quartz precipitation. Rapid cooling leaves the system super-saturated with quartz, and the excess concentration of silica in solution eventually reaches the solubility of amorphous silica at the lower temperature. Illite may also be formed in the hydrothermal experiments of which Figure 4 is an example.

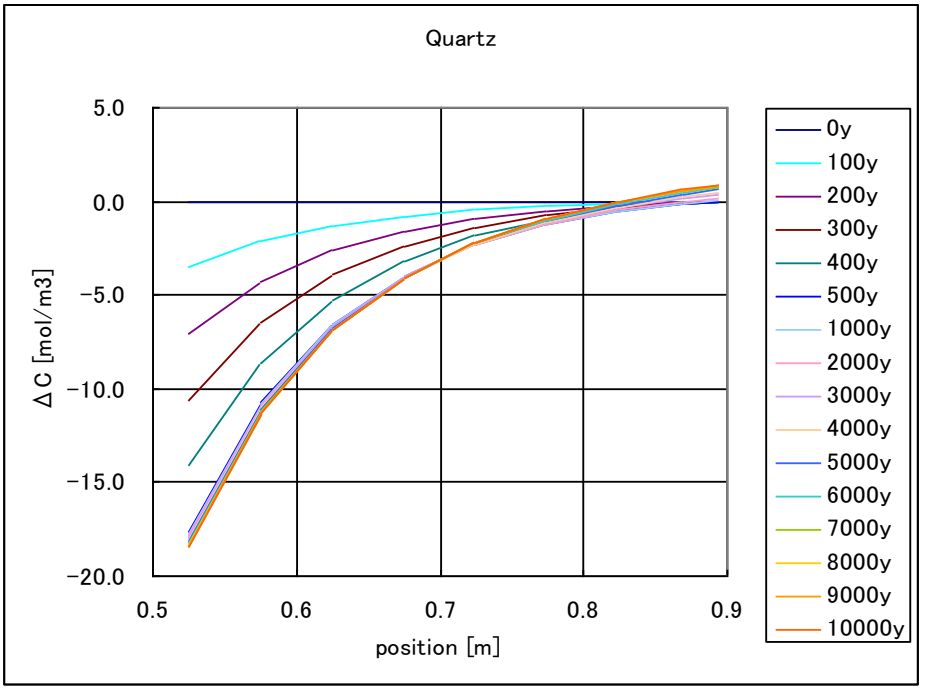

Figure 3: Evolution of quartz abundance profile (~10,000 y). Precipitation leading to cementation takes place in the outer, colder, 0.1 m part of the buffer according to Grindrod & Takase (Pusch and Yong, 2006).

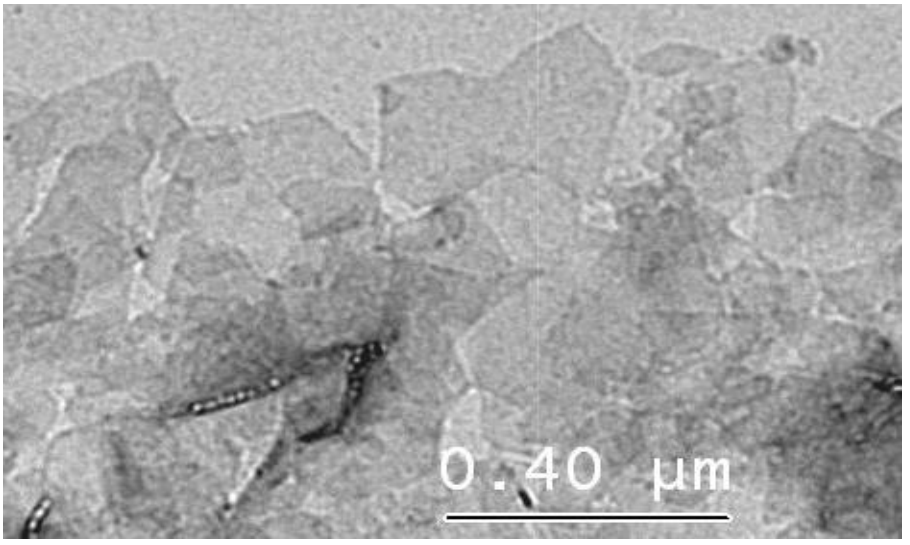

Figure 4: Neoformed pseudohexagonal particles in montmorillonite-rich MX-80 clay in contact with heater in a 3-year full-scale test of the KBS-3V concept at SKB's Äspö underground laboratory (After Kasbohm).

3. Recent clay degradation modelling

3.1 General

The mechanisms involved in conversion of smectite yielding illitization or smectitization have been investigated by Herbert et al. (2011) and Nguyen-Thanh (2012). These authors focused on the interaction of smectite-rich clay and iron identifying mineralogical reactions in laboratory experiments of compacted smectitic clays interacting with iron powder for simulating the contact of "buffer" clay bentonite with steel containers. These experiments included mechanical disturbance ("overhead rotation" on a large number of smectite-bearing clays and led to the conclusion that different smectite clays have different specific dissolution potentials. These investigators called smectite with low dissolution potential, "Sleeper", and smectite with high dissolution potential, "Sprinter". This can explain the different conversion paths for smectites of different origin: As long as the amount of dissolved Si does not exceed the Si-loss caused by through-flow of chemically "open" systems, the alteration process leads to "illitization", while smectitization is the dominating alteration mechanism if more Si is dissolved than lost. It means that clays composed of illite-smectite mixed layer minerals buffers dissolved Si and that the illite layers become converted to smectite. The process reduces the tetrahedral charge deficit which represents smectitization. The mechanism has been identified in mechanically agitated open systems and percolated batch experiments and in systems with no through-flow.

We will cite here a study of the mineralogy and chemical constitution of a Tertiary

Danish mixed-layer I/S Holmehus clay (Heilmannn-Clausen et al, 1985) and compare them with those of an internationally used reference clay from North-American Ordovician clay (Wyoming bentonite, MX-80).

3.2 Virgin material

The mineral composition of the two clays was made by X-ray diffraction analysis of randomly oriented powder of bulk samples and of oriented samples of < 2μm material in air-dried and ethylene-glycol-solvated forms. The study also included X-ray fluorescence (XRF)-analysis of 26 elements including LOI, and the cation exchange capacity (CEC) for determination of exchangeable Na, K, Mg and Ca. In addition, transmission electron microscopy (TEM)-examination of < 2 μm material was conducted for characterizing morphology and stack order, and for determining mineral formula (by TEM-EDX-analysis) for about 200 particles per sample. The latter included Fourier transform infrared spectroscopy (FT-IR)-examination for certifying XRD- and TEM-results respecting the octahedral and tetrahedral constitutions of the smectite component.

Bulk samples were milled in an agate mortar by hand to <32 μm for XRD-investigation using a Philips PW1710–BASIS X-ray diffractometer equipped with a Cu tube (Kα1,2 radiation) and a secondary monochromator. The processing of XRD-powder pattern included also Rietveld refinement for semi-quantitative determination of essential mineral components by applying BGMN-software (Bergmann et al., 1998; Ufer et al., 2008). Oriented specimens of the <2 μm fraction were analyzed by SIEMENS 106Theta/2Theta D5000-goniometer also equipped with a Cu tube (Kα1,2 radiation) as well as a 107 secondary monochromator. The WinFit program (Krumm, 1994) was used for XRD-diffractograms of oriented specimens (air-dried and ethylene-glycol treated) for getting line-profiles of clay minerals with broad and strongly overlapping XRD peaks and coherent scatter domains. Additionally, XRD patterns of oriented specimen were modelled by use of the Sybilla© software developed by Chevron™ (Aplin et al., 2006). This software program allows direct comparison between experimental and calculated XRD-profiles.

TEM investigations were carried out on the < 2μm fraction using a TECNAI G^2 20 electron transmission microscope of the Hanoi University of Science, Vietnam National University, Hanoi. It operated at 200 kV and was equipped with an EDAX energy-dispersive X-ray (EDX) system and a FEI Eagle™ 2k CCD TEM camera for characterization of morphology, crystal habit, element distribution and stack order evaluated by electron diffraction. Selected particles were analyzed chemically by EDX and the software toolkit of Kasbohm et al. (2011, 2013) used for calculation of mineral formula. The procedure in this toolkit considered the sum of equivalent charges of measured cations and its proportion to the theoretical total charge of assumed phase (e.g. 22 for illite; 28 for chlorite) following Köster (1977). In this context, illite, recognized by the TEM investigation, is here referred to as illite in the sense of Środoń et al. (1992), i.e. conforming to the following structural

formula of illite in sensu stricto:

$FIX_{0.89}$ $(Al_{1.85}$ $Fe_{0.05}$ $Mg_{0.10})$ $(Si_{3.20}$ $Al_{0.80})$ O_{10} $(OH)_2$

where FIX represents fixed K cations in the interlayer space. Furthermore, K- and/or charge-deficient dioctahedral micas, with tetrahedral Si ranging from 2.8 to 3.3 per $O_{10}(OH)_2$, are termed dioctahedral vermiculite. The acronyms "IS-ml" and "diVS-ml" refer to illite/smectite and dioctahedral vermiculite/smectite irregular interstratifications, respectively. Furthermore, smectitic layer-ratio (%S) was calculated using the TEM data bases on tetrahedral Al (Al^{IV}) according to Środón et al. (1992):

$$\%S = (100.38 \times (Al^{IV})^2 - 213 \times Al^{IV} + 100.25 \quad (6).$$

Rate/degree of alteration (Δ%S) was calculated by using differences in numbers of layers of smectitic reaction products (S% treated material) and smectitic layers of initial materials (S% virgin material).

$$\Delta\%S = \%S_{\text{treated material}} - \%S_{\text{original material}} \quad (7)$$

Based on the Δ%S yielded from TEM-EDX data, alteration of bentonite was empirically taken as "illitization" (Δ%S < 0, regardless of K-amount) or smectitization (Δ%S > 0). These processes were taken as Si-loss or Si-enrichment in comparison with initial materials (Herbert et al., 2011; Nguyen-Thanh, 2012), respectively.

FT-IR spectra were taken of KBr-tablets (10 g sample was mixed with 990 mg KBr Uvasol) with recording of the mid-infrared range (400 cm^{-1} to 4000 cm^{-1}) and Gaussian distribution functions applied for smoothing the spectra and providing exact values of the peak positions, intensity and area. The accuracy of the evaluations was R2 > 0.98. CEC was measured using Cu-triethylenetetramine (Cu-trien) in accordance with Dohrmann & Kaufhold (2009).

Mechanical disturbance by overhead rotation was made for simulate alteration of Holmehus clay (Herbert et al., 2011; Nguyen-Thanh, 2012) or more specifically, for removal of dissolved matter from the agitated particles. The test program comprised determination of the grain size distribution by sieving after crushing and milling air-dry raw material, and determination of hydraulic conductivity and swelling pressure of crushed and milled clay compacted in 50 mm oedometer cells for subsequent percolation with distilled water and 3.5% $CaCl_2$ solution in parallel tests. Furthermore, overhead rotation experiments in deionized water were made as a simple practical way of identifying mineralogical alteration processes.

3.3 Results

Mineral examination by XRD

The outcome of the XRD examination (cf. Figure 5) can be summarized as follows:

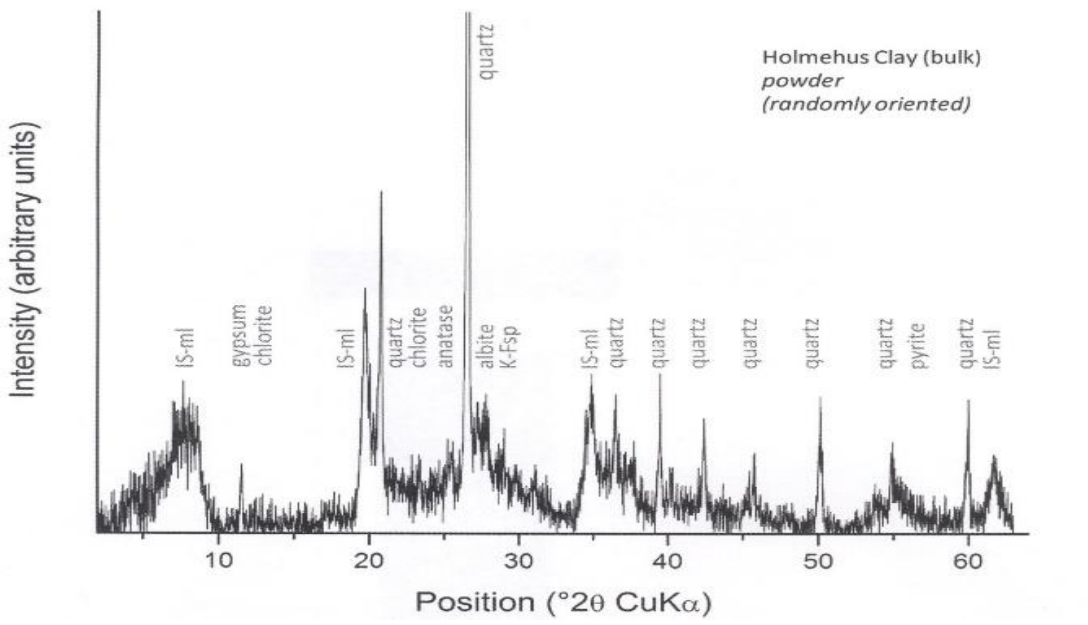

Figure 5. Holmehus bulk material (analysis by Kasbohm, Greifswald University, Germany).

1. The Holmehus IS clay is dominated by IS-ml (55%), muscovite of $2M_1$-polytype and quartz (Table 1). Small amounts of chlorite and feldspars were also found as well as traces of anatase, pyrite, gypsum and jarosite. The dioctahedral character of IS-ml and muscovite was proven by the occurrence of the (060)-interference at 0.1504 nm,

2. The XRD-pattern of oriented specimen (fraction < 2 µm) shows two fully expandable IS-ml phases (1.7 nm spacing for ethylene glycol saturation). The two phases consist of randomly interstratified illite-smectite mixed layer phases: IS-ml (Reichweite R0) with an illite layer probability of about 75%,

3. This IS-ml was characterized by a low K-deficit in the interlayer space of illite layers and also reduced charge of interlayer space in smectite. Furthermore, there is remarkable octahedral iron content originating in the illite layers. The second main group of randomly interstratified IS-ml was composed by 27% of illite layers with high K-amount in interlayer space (1.90 per $(OH)_4$ O_{20}) and also a high interlayer charge for smectite layers

(0.8 per $(OH)_4$ O_{20}). Illite and smectite layers have high iron contents in the octahedral sheet. Additional findings were iron-rich and high charged species of R1-ordered illite-smectite mixed layer structure with an illite layer probability of 40%, and Fe-rich and low charged discrete smectite as well as Fe-bearing chlorite (Table 2). The occurrence of quartz and probably traces of rozenite (0.447 nm) was noted.

The illite/smectite mixed-layer structure makes up 50-55 % by weight and the rest is specified in Table 1, which shows the corresponding properties of the MX-80 clay with 85% montmorillonite in the clay fraction.

Table1: Major accessory minerals in Holmehus and MX-80 clays. Weight percentages.

Clay	Muscovite $2M_1$	Chlorite	Quartz/ cristobalite	Plagioclase	K-feldspar	Calcite	Gypsum	Jarosite	Pyrite
Holmehus	10-20	<5	10-15	<5	5	3	2	2	0.3
MX-80	<2	<1	5-10	<3	<3	5	<1	-	0.2
Ratio of smectite layers (S%) is 60% in IS-ml= and 30% in diVS-ml.									

The evaluated element composition of Holmehus clay is compiled in Table 2, the corresponding data for MX-80 being shown for comparison. The illite/smectite mixed-layer structure makes up 50-55 % by weight. The MX-80 clay fraction has about 85% smectite (montmorillonite). Figure 4 shows FT-IR spectra of bulk material and of the clay fraction.

Table 2: Element data of bulk samples of Holmehus and MX-80 clays.

Element	SiO_2	Al_2O_3	Fe_2O_3	MgO	CaO	Na_2O	K_2O
Holmehus	58.6	15.3	6.5	2.2	0.7	1.4	2.8
MX-80	63.6	19.8	5.0	3.2	3.1	2.8	1.0

The cation exchange capacity of Holmehus clay was found to be 29.7-31.6 meq/100 g. For MX-80 the CEC has a typical average value of 90 meq/100 g.

3.3.1 Transmission electron microscopy (TEM)

The two kinds of mixed layer phases have two morphological forms: i) xenomorphic flakes (probably products of diagenetic alteration) and ii) laths with idiomorphic ends (probably detrital originating from weathered crust). Lath-like particles are enriched in fraction <0.5μm. Smectite of Na montmorillonite typically shows interwoven stacks of 3-10 10 Å lamellae and they appeared also in the Holmehus clay However, it also contained xenomorphic flakes as indicated in Figure 6, which represents one of the mixed-layer phases.

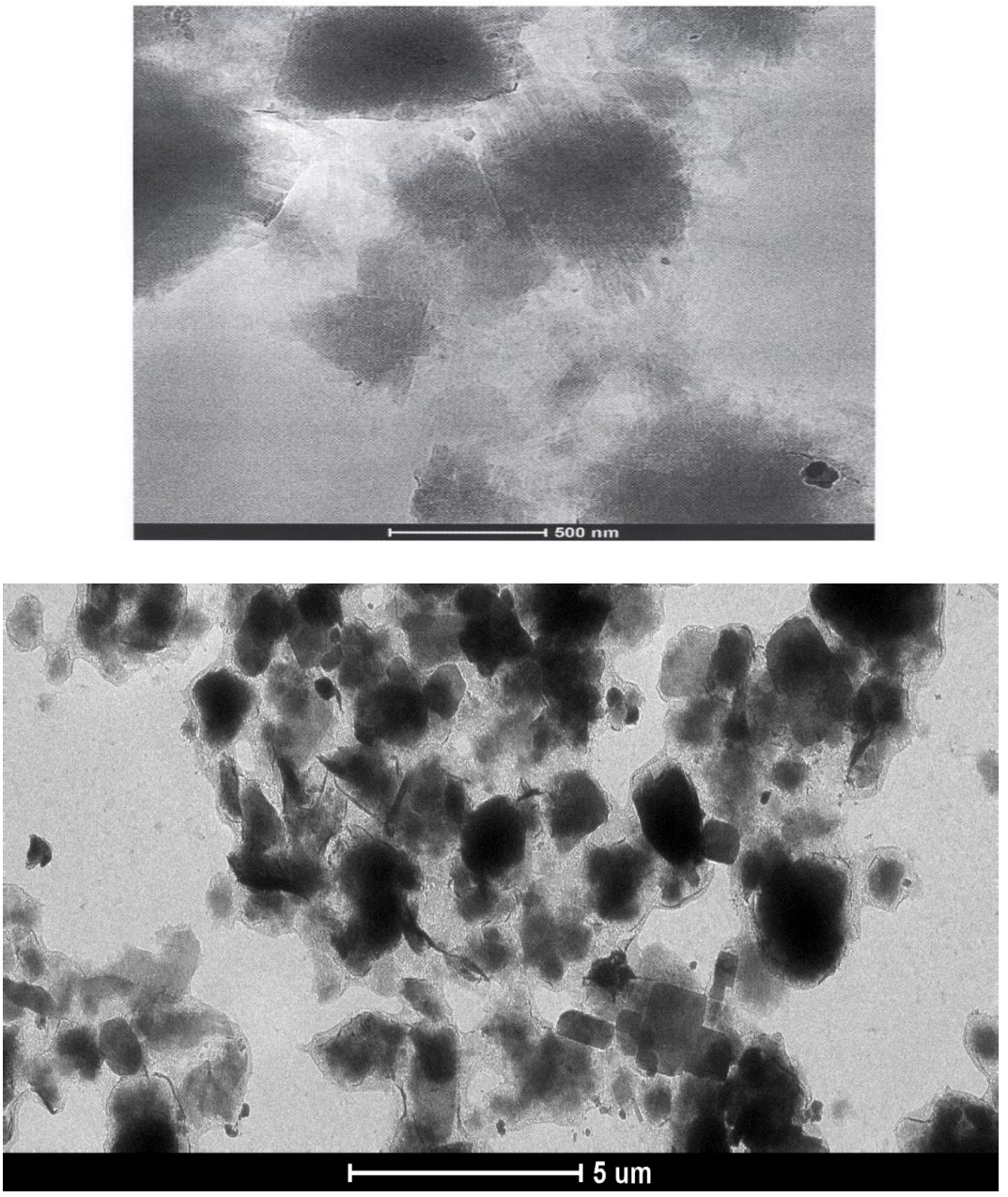

Figure 6: TEM micrographs of Holmehus clay. Upper: Lath-like illite-smectite mixed layer phases (magnification 20.000x). Lower: Mixed-layer IS particles in the coarser part of the clay fraction (By Kasbohm, Greifswald University, Germany).

The TEM-EDX element analyses showed that the IS-ml structures make up 45 frequency-% and the diVS-ml phases make up 15 frequency-% in Holmehus clay. The rest was found to consist of quartz (18 frequency-%) and Fe- as well as Ti-phases. The content of smectite layers (S%) in IS-ml is 60% and for the diVS-ml it is 30%. The two mixed-layer series is characterized by Fe-rich octahedral sheets. They can be distinguished by the remarkably different tetrahedral compositions.
Mixed-layer phases identified by TEM were compared with XRD fitting results. The component with 27% illite layer probability and 40% illite layer probability have high K-amounts in the illite layers and high interlayer charge in smectite layers. The TEM-data respecting octahedral iron and smectite layer probability showed remarkable differences from those obtained from modelling of XRD-spectra. The TEM-derived iron contents were higher and the values of smectite layer probability were lower than expected from XRD-pattern modelling. Iron may be an iron oxide crust surrounding the particles.

3.4 Expected transformation of Holmehus clay as engineered barrier for isolating

3.4.1 General

The most important matter concerning use of smectitic clays for isolating hazardous waste like radioactive rest products is that the clay seals must operate according to given criteria for a given time that can be from a few hundred years to a hundred thousand years. It has been in focus for a long time and led to the conclusion by various investigators that smectite-rich clays like the commercial MX-80 clay will stay largely intact for very long periods of time under the hydrothermal conditions that will prevail in repositories (Pusch & Yong, 2006). The threat is basically that exposure of the clay to temperatures of up to 150ºC for several decades in salt environment can cause dissolution of the swelling minerals and thereby loss of tightness, expandability and self-sealing ability (Pusch et al., 2013). Precipitation of dissolved elements can take place in the subsequent cooling period by which cementation will occur, causing further reduction of the expandability that has to be preserved for maintaining tight contact with the surroundings. These can be rock or concrete constructions, which makes it necessary to consider chemical interaction of clay and cement and degradation of both (Pusch et al., 2003).

3.4.2 Hydrothermal impact on Holmehus clay

Applying the “Specific Dissolution Potential”- and “Si-buffer”-concepts of Herbert et al. (2011) and Nguyen-Thanh (2012), Holmehus clay has shown only the low dissolution potential of “Sleepers” by low-intensity mechanical treatment while increased energy input changed the Holmehus clay to become a “Sprinter”. The high amount of dissolved Si exceeded the loss of this element by the treatment, hence generating more smectite. The comparison with Friedland clay indicated that further increase of the energy input (60 rpm) would continue the smectitization process in Holmehus clay.
Smectitization of Holmehus clay is hence expected to be the main alteration process even under the high temperature near the HLW containers in a repository because of the low flow rate of porewater in the barrier system as indicated by experiments with native iron in contact with compacted MX-80 bentonite and Friedland clay at 90°C (Herbert et al.

2011).

3.4.3 Expected behaviour of Holmehus clay by hydrothermal experiments under thermal gradients

Xiaodong et al. (2011) exposed confined MX-80 bentonite and samples of the Holmehus-like Friedland clay to considerable thermal gradients that drove porewater through the tested samples. This caused salt accumulation in the most heated parts and differences in density in all parts. In contrast to Friedland clay, MX-80 clay had undergone considerable changes, particularly in the form of a very significant loss of swelling pressure and a rise in hydraulic conductivity by 100 times in the hottest part. The central and cold parts were also markedly changed with respect to conductivity but they retained their expandability. The swelling pressure of the mixed-layer clay had dropped notably in the hottest part but only slightly in the central and cold parts. The hydraulic conductivity of the hot part was about 50 times higher than of virgin clay but remained unchanged in the central and cold parts. The most heated clay parts had undergone slight dissolution, and minor precipitation of siliceous material can have taken place causing cementation and partial loss of expandability. Copper, forming the heated ends of the hydrothermal cells, had dissolved and migrated by more than a millimeter into the clay by diffusion in a few weeks (Kasbohm et al. 2013).

The small degrading impact of the hydrothermal treatment on MX-80 bentonite respecting the mineral composition shows that it performed as "Sleeper" and that the obvious cementation by precipitated Si as documented by considerable stiffening in compression tests, suggests that the tetrahedral Si in montmorillonite offered only a low Si-buffer capacity. Such impact on Friedland clay was significantly lower because of its higher Si-buffering capacity. Experiments by Herbert et al (2011) with Friedland clay have shown that the swelling pressure and permeability of this clay and MX-80 bentonite with admixed native Fe at low concentration for 25°C, 60°C and 90°C are less permeable when the swelling pressure increases but that this is no longer the case for high Fe0-concentration and temperatures at 90°C. Cemented aggregates caused decreasing permeability by clogging voids.

Breakage of cemented aggregates by mechanical agitation raised the permeability without decreasing the swelling pressure. In the light of the experiments the hypothesis of more effective Si-buffering of mixed-layer S/I clays, one concludes that the Holmehus clay, being similar to the Friedland clay, will perform acceptably as buffer clay because of its character as "Sleeper".

4. Overall conclusions

The general conclusion from this contemplation is that smectite/illite mixed-layer clays of the presently examined kind have sufficiently good physical properties to qualify as "buffer" isolation of hazardous waste including highly radioactive rest products like spent reactor fuel. They can be regarded as weathered bentonites representing an intermediate stage between freshly formed montmorillonite and very old bentonites that have undergone complete conversion to non-expandable clay minerals like the Ordovician clays on Gotland which underwent consolidation under very high overburden pressure and temperature (Pusch et al., 2011). The

impact on the chemical integrity of Holmehus clay of the hydrothermal conditions in a repository is believed to be similar to but less extensive than those of competing smectite-rich clays like MX-80.

The most important results reached in the study concerns the mineral stability and the role of dissolved silica under hydrothermal conditions. Firstly, different smectite clays have specific dissolution potentials. Smectite with low dissolution potential behave as "Sleeper" and retain their expandability and tightness for very long times while smectite with high dissolution potential is a "Sprinter" and undergoes early and significant convergence to non-expandable forms. IS-ml bearing clays like Holmehus clay compensate their fast alteration by smectitization. This smectitization coupled with the high Si-buffering capacity of IS-ml bearing clays improve the barrier performance concerning swelling pressure and permeability also by avoiding of cementation of particles.

References

[1] Aplin, A.C., Matenaar, I.F., McCarty, D.K. and van der Pluijm, B.A. (2006). Influence of mechanical compaction and clay mineral diagenesis on the microfabric and pore scale properties of deep-water Gulf of Mexico mudstones. Clays & Clay Minerals, 54, 500-514. DOI: 10.1346/CCMN.2006.0540411.

[2] Bergmann, J., Friedel, P. and Kleeberg, R. (1998). BGMN - a new fundamental parameter based Rietveld program for laboratory X-ray sources, its use in quantitative analysis and structure investigations. CPD Newsletter, 20, 5–8.

[3] Dohrmann, R. and Kaufhold, S. (2009). Three new, quick CEC methods for determining the amounts of exchangeable calcium cations in calcareous clays. Clays and Clay Minerals, 57(3), 338-448. DOI: 10.1346/CCMN.2009.0570306

[4] Grindrod, P. and Takase, H. (1993). Reactive chemical transport within engineered barriers. In: Proc. of the 4th Internat. Conf. on the Chemistry and Migration Behaviour of Actinides and Fission Productsin the Geosphere, Charleston, SC, Oldenburg Verlag, 1994.

[5] Heilmann-Clausen, C., Nielsen, O.B. and Gersner, F. (1985). Lithostratigraphy and depositional environments in the Upper Paleocene and Eocene of Denmark. Bulletin of the Geological Society of Denmark, 33/3-4, 287-323.

[6] Herbert, H., J., Kasbohm, J., Nguyen, T.L., Meyer, L., Hoang, T.M.T. and Xie, M. (2011). Fe-459 Bentonite - Experiments and Modelling of the Interactions of Bentonites with Iron. GRS - 295, ISBN 978-3-939355-72-4, 292 pp.

[7] Kasbohm, J., Tarrah, J. and Henning, K.-H. (2002). Transmissionselektronen-mikroskopische Untersuchungen an Feinfraktionen der Ringversuchsprobe "Ton Stoob". pp. 71–84, in: Beiträge zur Jahrestagung Wien, 18.-20.9. 2002 (Berichte der Deutschen Ton- und Tonmineralgruppe e.V. Band 9).

[8] Kasbohm, J., Pusch, R., Nguyen-Thanh L. and Hoang-Minh T. (2013). Lab-scale performance of selected expandable clays under HLW repository

conditions. Environmental Earth Sciences, 69(8), 2569-2579. DOI: 10.1007/s12665-012-2085-1

[9] Köster, H.M. (1977). Die Berechnung kristallchemischer Strukturformeln von 2:1 – Schichtsilikaten unter Berücksichtigung der gemessenen Zwischenschichtladungen und Kationenaustauschkapazitäten, sowie die Darstellung der Ladungsverteilung in der Struktur mittels Dreieckskoordinaten. Clay Minerals, 12, 45–54.

[10] Krumm, S. (1994). WINFIT 1.0 - A Computer Program for X-ray Diffraction Line Profile Analysis. Acta Universitatis Carolinae Geologica, 38, XIIIth Conference on Clay Mineralogy and Petrology, Praha, 253-261.

[11] Nadeau, P.H., Wilson, M.J.,McHardy, W.J. and Tait, J.M. (1984). Interparticle diffraction. A new concept for interstratified clays. Clay Minerals, 19,757-769.

[12] Nguyen-Thanh, L.(2012). Mineralogical Characterization of Fe-driven Alteration in Smectites. Ph.D. thesis, Ernst-Moritz-Arndt-University Greifswald, Germany, 213 pp.

[13] Pusch, R. (1993). Evolution of models for conversion of smectite to non-expandable minerals. Swedish Nuclear Fuel and Waste Management AB. SKB Technical Report TR-93-33, SKB, Stockholm, Sweden-

[14] Pusch, R., and Yong, R.N. (2006). Microstructure of smectite clays and engineering performance. Francis & Taylor, ISBN10: 0-415-36863-4.

[15] Pusch, R. (2008). Geological Storage of Radioactive Waste. Springer Verlag, Berli-Heidelberg.

[16] Pusch, R., Yong, R.N. and Nakano, M. (2011). High-level Radioactive Waste (HLW) Disposal. WIT Press, Southampton, Boston.

[17] Pusch, R., Mohammed Hatem M., M., Kasbohm, J., and Knutsson, S. (2013). Roles of clay and concrete in isolating High-level radioactive waste in very long holes. International Journal of Research and Reviews in Applied Sciences, 16(2), 263-273.

[18] Pusch, R. (2015). Bentonite Clay – Environmental Properties and Applications. CRC Press, Taylor & Francis, London and New York.

[19] Środón, J., Elsass, F., McHardy, W.J. and Morgan, D.J. (1992). Chemistry of illite-smectite inferred from TEM measurements of fundamental particles. Clay Minerals, 27, 137-158.

[20] Ufer, K., Stanjek, H., Roth, G., Dohrmann, R., Kleeberg, R. and Kaufhold, S. (2008). Quantitative phase analysis of bentonites by the Rietveld method. Clays and Clay Minerals, 56(2), 272-282. DOI: 10.1346/CCMN.2008.0560210

[21] Xiaodong, L., Prikryl, R. and Pusch, R. (2011). THMC-testing of three expandable clays of potential use in HLW repositories. Applied Clay Science, 52, 419-427. DOI: 10.1016/j.clay.2011.03.021